
**Journal of Macromolecular Science, Part A**
Publication details, including instructions for authors and subscription information:
http://www.informaworld.com/smpp/title~content=t713597274

# Ion Tunneling in Polymeric Solid Electrolytes for Batery and Electrochromic Display in the Dry State

Eishun Tsuchida[a]
[a] Department of Polymer Chemistry, Waseda University, Tokyo, Japan

**To cite this Article** Tsuchida, Eishun(1988) 'Ion Tunneling in Polymeric Solid Electrolytes for Batery and Electrochromic Display in the Dry State', Journal of Macromolecular Science, Part A, 25: 5, 687 — 704
**To link to this Article: DOI:** 10.1080/00222338808053393
**URL:** http://dx.doi.org/10.1080/00222338808053393

J. MACROMOL. SCI.–CHEM., A25(5-7), pp. 687-704 (1988)

# ION TUNNELING IN POLYMERIC SOLID ELECTROLYTES FOR BATTERY AND ELECTROCHROMIC DISPLAY IN THE DRY STATE

EISHUN TSUCHIDA

Department of Polymer Chemistry
Waseda University
Tokyo 160, Japan



## ABSTRACT

Polymeric solid electrolytes which show bi- or single-ionic tunneling were prepared, and their unique ion conduction was applied for the design of some devices. Poly[(oligooxyethylene) methacrylate]/MX hybrids and poly[(oligooxyethylene) methacrylate-*co*-methacrylic acid alkali metal salts] were prepared as typical models of those tunneling systems. These showed ionic conductivities above $10^{-5}$ and $10^{-7}$ S/cm at room temperature, respectively. An all-solid-state electrochromic display and a dry battery were prepared with these polymeric solid electrolytes. The all-solid-state electrochromic display showed excellent coloring and bleaching response by 1-3 V. The all-solid-state battery showed $V_{oc}$ = 3.1 V stability for over 2 weeks. Their characteristics as well as their mechanism are also reported.

## INTRODUCTION

Ion migration is a comprehensive phenomenon but one of the most important processes for the transmission of information in biological systems as well as for electrochemical reactions. However, this process has been limited to solutions. Matrices which enable ion tunneling in the solid state, called solid elec-

trolytes, are thus recognized to be worthy of study. A steep increase of interest, especially in polymeric systems, has developed in this decade. Polymeric solid electrolytes have great advantages, such as high ionic conductivity, ion selectivity, good processability, and transparency; they can be used in thin films, dry systems, etc.

Much work has been carried out to design matrix polymers, such as an organic polar polymer/additive system [1-3], polyethers [4-15], poly(ethylene succinate) [16, 17], poly(ethyleneimine) [18], and poly(alkylene sulfide) [19]. These polymeric solid electrolytes mixed with $LiClO_4$ show conductivities of $10^{-5}$ to $10^{-9}$ S/cm at 25°C, depending on the characteristics of the polymer matrix. The author has already demonstrated not only high ionic conductivity (over $10^{-5}$ S/cm at room temperature) with a comblike polymer [13, 20] but also with a polymeric solid electrolyte (over $10^{-7}$ S/cm of cation single-ionic conductivity) [14, 15]. Those with the advantages mentioned above are expected to be applicable to all-solid-state batteries, ionic sensors, condensers with high capacity, and electrochromic display.

In this paper the author reports on the construction of an all-solid-state electrochromic display and a battery with polymeric solid electrolytes possessing a suitable ion conduction profile.



## EXPERIMENTAL

### Polymeric Solid Electrolytes

Methacryloyl oligo(oxyethylene) monomethyl ether ($MEO_n$) derivatives with $n$ values of 3, 7, 12, and 17 were prepared according to Scheme 1 [13].

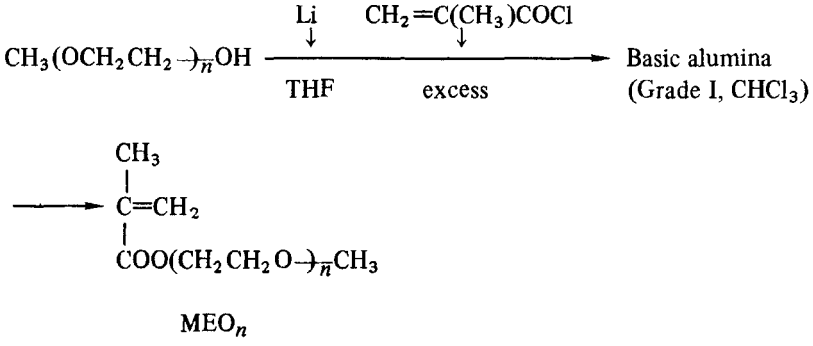


SCHEME 1.

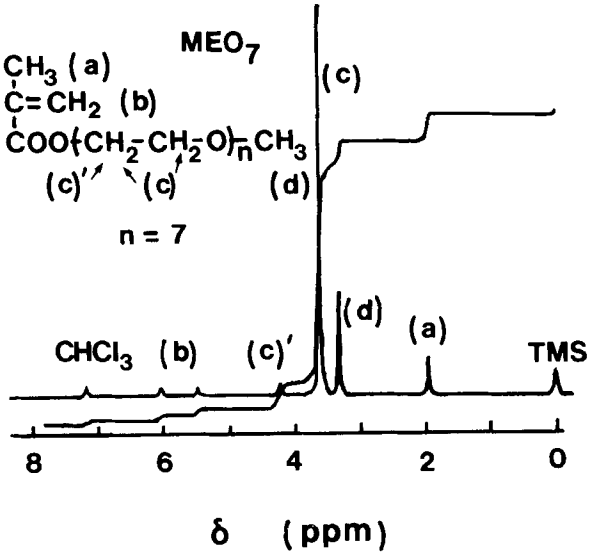


FIG. 1. $^1$H-NMR spectrum of $MEO_7$ in $CDCl_3$ at 25°C.

The structure has been mainly confirmed by $^1$H-NMR spectra, one example of which is shown in Fig. 1. Polymeric solid electrolytes were prepared by the following procedure. A methanolic solution of $MEO_n$ was mixed with an alkali metal salt or a methacrylic acid alkali salt and 1.0 mol% AIBN with respect to the total vinyl monomers. The resultant solution was placed on a Teflon plate, and the casting solvent was allowed to evaporate under dry argon flow at 60°C for 1 d. The resulting product was further evacuated at 80°C for another day for thermal polymerization and complete drying.

### Other Chemicals

All solvents were stored over Molecular Sieves and distilled before use. All alkali salts were purified by ordinary purification methods. For example, $LiClO_4$ was dried at 160°C *in vacuo* for 2 d. Methacrylic acid alkali salts were prepared by neutralization of methacrylic acid with alkali hydroxides in dry methanol, and were then precipitated by pouring the methanol solution into dry acetone.

### $WO_3$ Electrode Coating

$WO_3$ was coated by electron beam evaporation (10 kV and 30 mA) of $WO_3$ powder onto an ITO electrode (7 $\Omega/cm^2$) under vacuum below $3.7 \times 10^{-2}$ Pa. The deposition rate was 5 A/s, and the deposition angle was varied within 60° with a planetary rotation. The substrate was maintained at 100°C. The thickness of the $WO_3$ films was monitored with a multiple interferometer and controlled to be around 2 $\mu$m. Electron beam diffraction analysis (50-100 kW) revealed that the coated $WO_3$ films were amorphous.

### Measurements

All measurements were carried out in a dry box under a dry argon atmosphere to avoid moisture.

Alternating current (1 V) ionic conductivity of the hybrid films was measured with a multifrequency LCR meter, Yokogawa-Hewlett Packard Model 4274A, in a frequency range of $10^2$ to $10^5$ Hz. A disk sample with a diameter of 10 mm was sandwiched between metallic lithium electrodes or stainless electrodes. The ionic conductivity was estimated from the complex impedance plane plots by computer curve fitting [21]. The temperature dependence of the conductivity was analyzed under a dry argon atmosphere by an ac measurement technique with a temperature-controlled apparatus from 0 to 80°C. Metallic lithium electrodes or platinum electrodes were used for dc (3 V) conductivity measurements with a Kikusui dc power supply (Model PAC7-10), a Kikusui millivoltammeter (Model 115) and a Keithley solid-state electrometer (Model 610C) and recorded with a pen recorder, National VP-65-11A. The discharge characteristics of the all-solid-state battery were also evaluated. Details of the instrumentation have been described elsewhere [13].

Coloring and bleaching of the electrochromic display (ECD) were carried out by applying a dc bias across the cell with a dc voltage generator ranging from 0 to 3 V. Changes in the optical density for the cell corresponding to coloring and bleaching were measured by a double-beam UV/VIS spectrophotometer, Hitachi-320 spectrophotometer, with potential control apparatus. Electricity was measured with a digital coulombmeter, Nikko Keisoku NDCM-1.

## RESULTS AND DISCUSSION

### Bi-Ionic Tunneling in Polymeric Solid Electrolytes

Poly(oligooxyethylene) methacrylate containing $LiClO_4$ salt showed an ionic conductivity of $2.2 \times 10^{-5}$ S/cm at room temperature, as shown in Fig. 2.

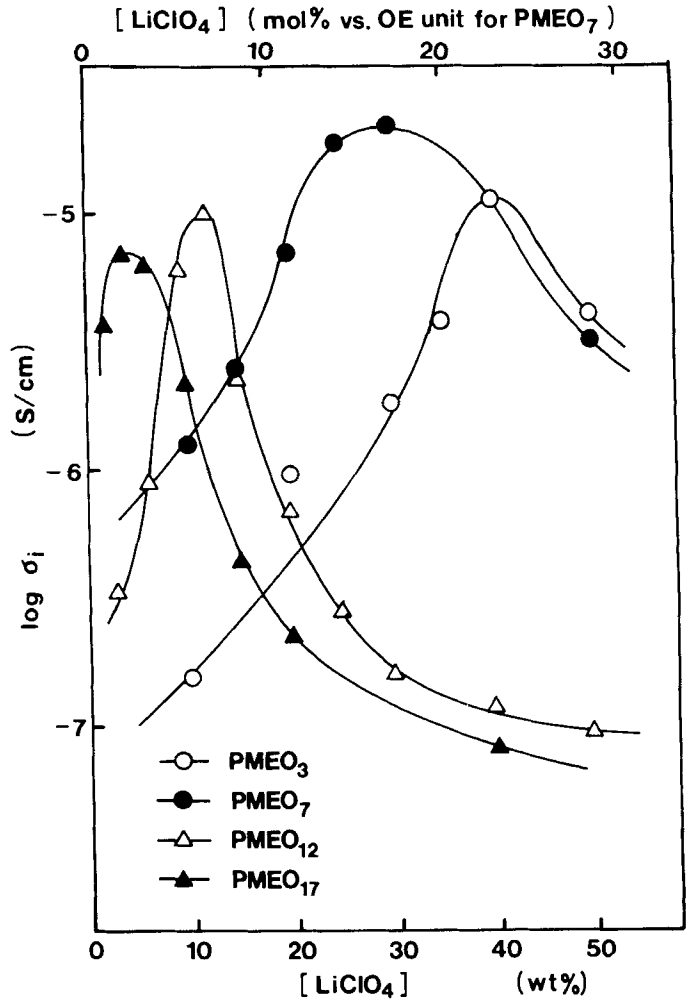


FIG. 2. Salt content dependence of ac (1 V) ionic conductivity for $P(MEO_n)/LiClO_4$ hybrid films at 25°C.

This is similar to that observed in the corresponding fluid solution system of $PEO_7/LiClO_4$. When the $LiClO_4$ concentration increased, the number of carrier ions also increased, but the microviscosity rose even more because of the interaction between lithium ion and ether oxygen in the hybrid film, caus-

ing a decrease in the mobility of the carrier ions. The increase of the microviscosity should probably be greater for $P(MEO_n)$ hybrids with larger $n$. The stronger interchain interactions between longer sidechains by the crosslinking-like effect of the added lithium cations further increased the microviscosity. The $P(MEO_n)/LiClO_4$ hybrid system with higher $n$ values exhibited higher ionic conductivity at low $LiClO_4$ content [13]. The descending order of ionic conductivities, $P(MEO_{17}) > P(MEO_{12}) > P(MEO_7) > P(MEO_3)$, is ascribable to the different number of dissociated carrier ions even at the same content of $LiClO_4$.

$P(MEO_7)$/MSCN (M = Li, Na, or K) hybrid films were prepared, and their ionic conductivities were measured. The ionic conductivity in low salt concentration was in the order KSCN > NaSCN > LiSCN, while at high salt concentration it was KSCN > LiSCN > NaSCN. The reason for this phenomenon is that $P(MEO_7)$/NaSCN has a higher $T_g$ than the others at high salt concentration, suggesting that the microviscosity increased for the $P(MEO_7)$/NaSCN hybrid and the carrier mobility of the sodium ion decreased [15].

The temperature dependence of the ionic conductivity for $P(MEO_7)$/MSCN hybrid films showed curved Arrhenius plots (Fig. 3), suggesting that the ionic tunneling in these films obeyed the WLF model rather than the Arrhenius model. This is typical for ion migration in a solid polymer matrix [20]. Thus, it is clear that the ion tunneling in the hybrid films is affected by the segmental motions of the polymer matrix.



### Single-Ionic Tunneling in Polymeric Solid Electrolyte

Bi-ionic conduction is an intrinsic property of almost all polymeric solid electrolytes, and dc conductivity is therefore decreased by long dc polarization, even though alkali metal nonblocking electrodes are employed [13, 20]. Such a decrease of dc ionic conductivity would be quite inconvenient when polymeric solid electrolytes are used in devices operating under dc polarization. Therefore, it is important to develop single-ionic conductors. Single-ionic conduction can take place only in solids. Therefore, methacrylic acid alkali salts (MAM, M = Li, Na, or K) were copolymerized with $MEO_7$, facilitating salt dissociation and ion migration [14, 15]. Ac ionic conductivities for $P(MEO_7$-MAM) films are shown in Fig. 4. Increasing MAM concentration led to conductivity maxima, and the salt concentration for maximum conductivity rises in the order of MAK < MANa < MALi. This phenomenon depended strongly on the dissociation energy of the salt. Temperature dependence of the ionic conductivities for $P(MEO_7$-MAM) films, shown in Fig. 5, indicates that the ionic conduction mechanism for the single-ionic systems also obey WLF behavior as in bi-ionic systems.

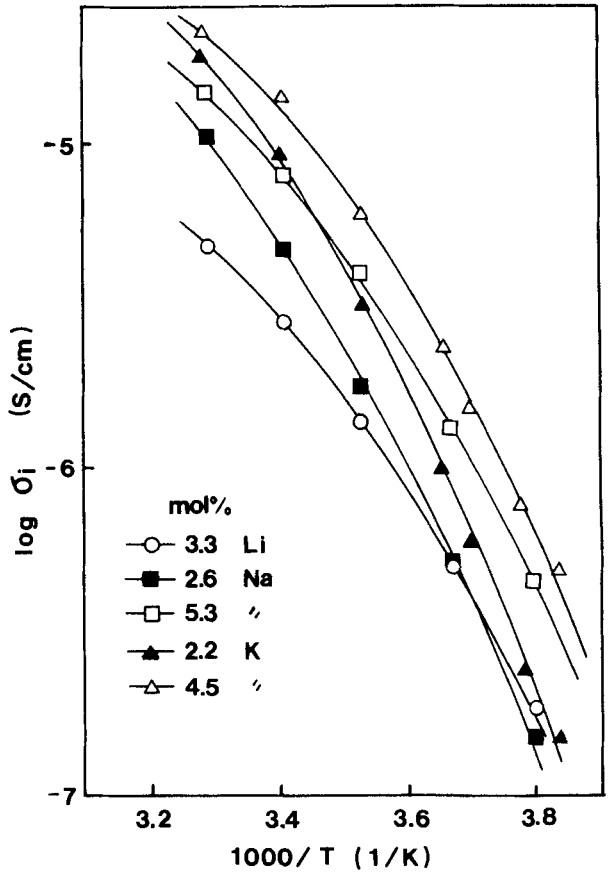


FIG. 3. Temperature dependence of ac (1 V) ionic conductivity for $P(MEO_7)$/MSCN hybrid films.

The time dependence of ionic conductivity of a $P(MEO_7$-MALi) film sandwiched between metallic lithium electrodes is shown in Fig. 6 (Curve A). The ionic conductivity of the $P(MEO_7$-MALi) film showed excellent stability, suggesting that it is a single-ionic conductor. The cation transport number has already been measured by the isothermal transient ionic-current method, called the "time-of-flight" method [22]. After applying 5 V ac for 10 h at 80°C with platinum electrodes, inversed bias polarity was applied to measure the transient ionic current. The time dependence of the current through the film,

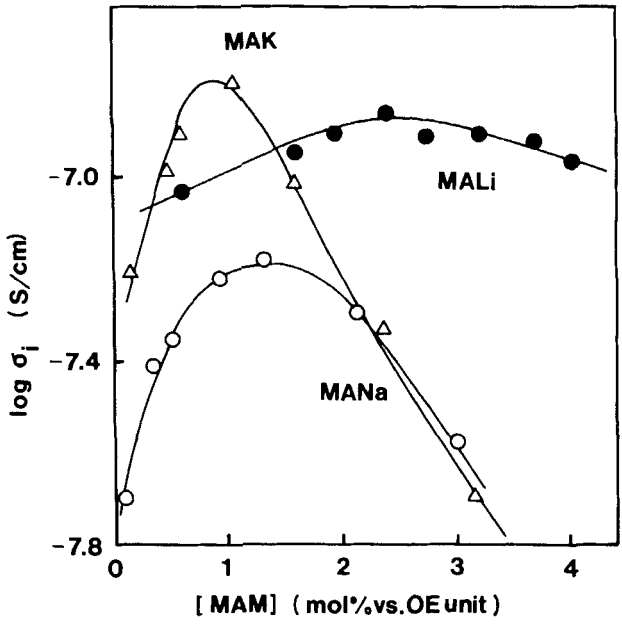


FIG. 4. Salt content dependence of ac (1 V) ionic conductivity for P($MEO_7$-MAM) films at 25°C.



as shown in Fig. 6 (Curve B), shows a peak at 10 s and a broad one at about 12 min, corresponding to the migration of the cation carrier sheet and the anion contribution, respectively. The carrier mobility can therefore be determined from

$$\mu = d^2/\tau V, \tag{1}$$

where $\mu$, $V$, and $\tau$ are carrier mobility, applied voltage, and time for the maximum current, respectively. The calculated transport number of $Li^+$ was found to be 0.99 for this film, indicating that P($MEO_7$)/MALi film is a single-ionic conductor.

### Application of Bi-Ionic Conductors to All Solid-State Display

An electrochromic display (ECD) cell with solid-state electrolyte is shown in Fig. 7 [23]. $WO_3$ electrode and an ITO electrode coated with a P($MEO_7$)/

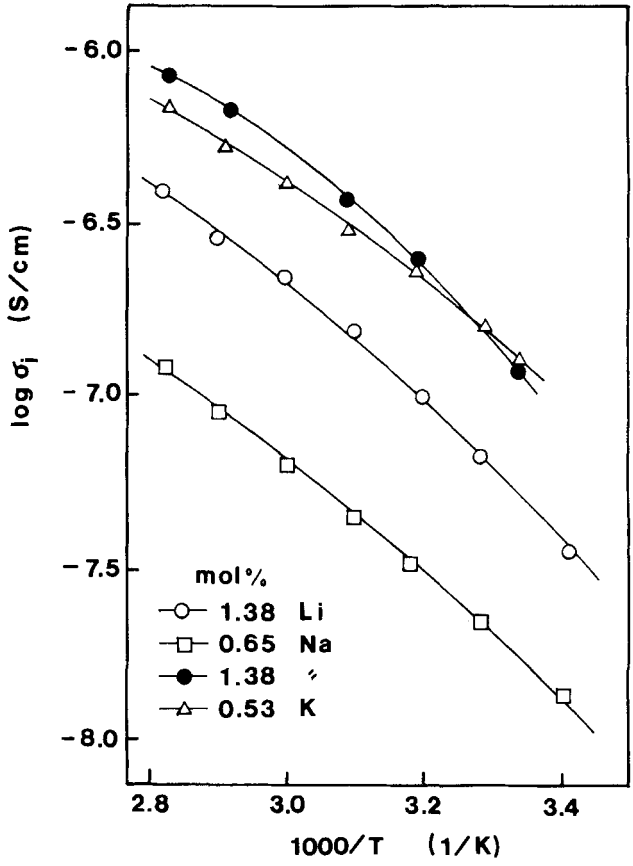


FIG. 5. Temperature dependence of ac (1 V) ionic conductivity for P($MEO_7$-MAM) films.

$LiClO_4$ hybrid film, which showed high ionic conductivity above $10^{-6}$ S/cm, were placed in contact under light pressure in a dry argon atmosphere. The ECD cell was sealed with epoxy resin to protect it from moisture. The thickness of the polymeric solid electrolyte was controlled at several tens of $\mu$m.

When the UV/VIS absorbance spectra for the coloring and bleaching state of the ECD were measured by a UV/VIS spectrophotometer, the maximum difference of the absorbance between the coloring and bleaching state was found at 800 nm. Therefore, EC characteristics were evaluated as the optical

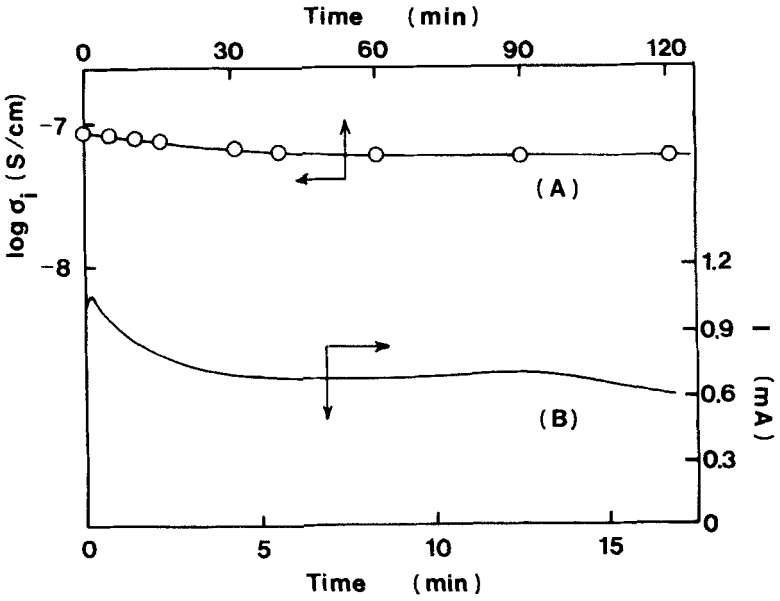


FIG. 6. (A) Time dependence of dc (3 V) ionic conductivity for P($MEO_7$-MALi) film at 25°C. (B) Transient ionic current for P($MEO_7$-MALi) film at 80°C. Film thickness: 23 $\mu$m.



density change at 800 nm. The coloring and bleaching behaviors at constant voltages ($0 < V < 3$) are shown in Fig. 8. No decomposition of constituents was found under these applied voltages. However, when more than 3.5 V was applied across the ECD cell, its constituents were degradated and less reliable reproducibility of coloring and bleaching was observed.

During the coloring and bleaching processes, the rate of the optical density change rose with the applied voltage. It was noted that the bleaching under 1 V dc bias was slower than that for 2 or 3 V. Apparently the required voltages for coloring and bleaching were determined by the total resistance of the cell because this cell has two electrodes, and the coloring and bleaching processes are based on the electrochemical intercalation of lithium ions in the $WO_3$ electrode. The voltage drop in this cell was mainly attributed to the higher resistivity of polymeric solid electrolyte compared to that of the electrolyte solution. Therefore, its critical voltage for the bleaching reaction should lie between 1 and 2 V, as shown in Fig. 8. The coloring and bleaching

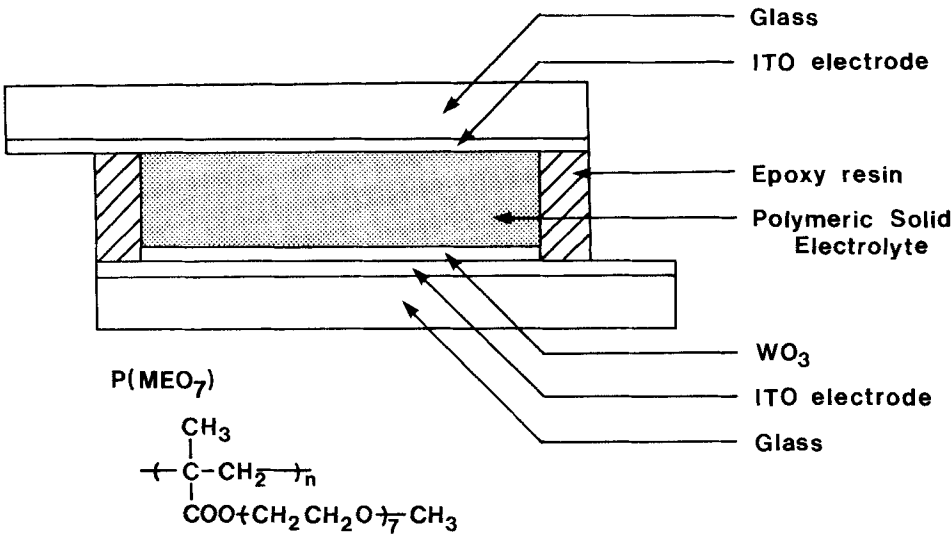


FIG. 7. Cell construction of all-solid-state electrochromic display.



behavior was not changed by repeating these procedures several times unless it fell below 3 V. At 0 V (open circuit), about 90% of the initial coloring state of the ECD cell was maintained after 40 h.

Efficient coloring for ECD is one of the important characteristics for commercial use. The relationship between the amount of the injected charge and the optical density change of the ECD is shown in Fig. 9. The theoretical data, i.e., all injected $Li^+$ ions inserted into $WO_3$ layer, considered to control the coloring and the experimental data for the electrolyte solution system (propylene carbonare/$LiClO_4$), are also shown in Fig. 9. The all-solid-state ECD gave a linear relationship, suggesting that the coloring behavior of this cell was based on injection of $Li^+$ into the $WO_3$ layer. However, the coloring efficiency for the ECD was higher than that for the propylene carbonate/$LiClO_4$ solution system. This higher efficiency for all-solid-state ECD was explained by the difference of the $Li^+$ transport number between $P(MEO_7)/LiClO_4$ hybrid film ($\mu_+ = 0.83$) [24] and propylene carbonate/$LiClO_4$ solution ($\mu_+ = 0.3$) [25].

Coloring and bleaching behavior deeply depended on $Li^+$ tunneling because the electron migration was so fast compared with $Li^+$. Coloring was mainly regulated by the interfacial resistance between $WO_3$ and the $Li^+$-injecting con-

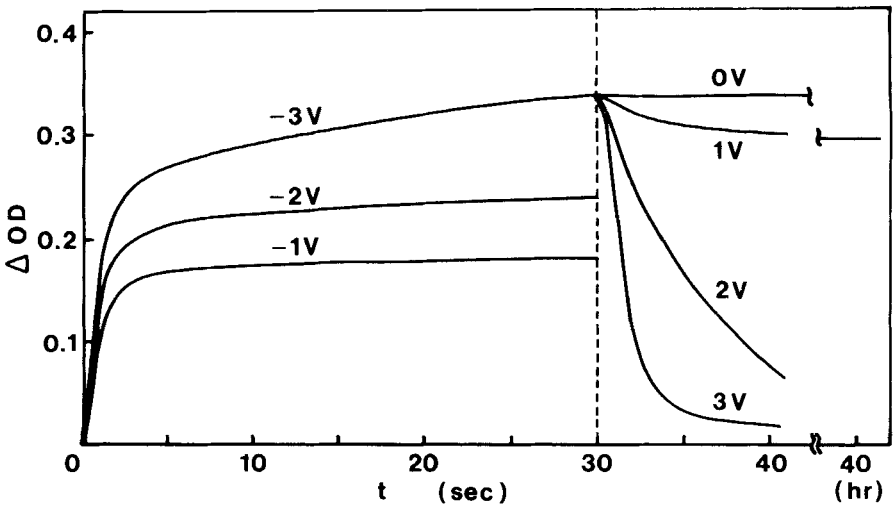


FIG. 8. Electrochromic response of all-solid-state electrochromic display under various voltages.



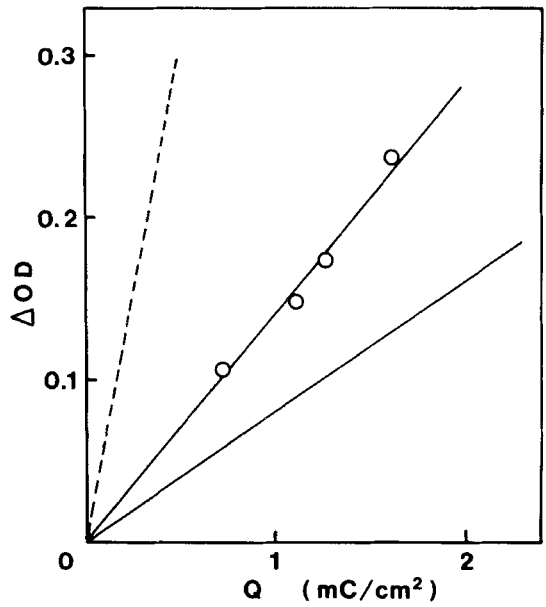


FIG. 9. Optical density change as a function of injected charge for all-solid-state electrochromic display. (- -): Theoretical value. (—○—): Experimental value for this polymeric system. (——): Experimental value for propylene carbonate/$LiClO_4$.

tact, whereas bleaching was regulated by $Li^+$ transport in the $WO_3$ layer. Theories of both coloring [26] and bleaching [27] were developed by Mohapatra and Faughnan for the electrolyte solution system. For the coloring process, the flowing current is described by

$$J_c = \pi^{-1/2} nFD_0^{1/2} C^0 t^{-1/2}, \tag{2}$$

where $n$, $F$, $D_0$, and $C^0$ are the number of electrons participating in the reduction, the Faraday constant, the diffusion coefficient, and the concentration of the redox species ($Li^+$), respectively. This equation indicates that the coloring current $J_c$ is a linear function of $t^{-1/2}$.

For the bleaching process, the flowing current is described by

$$J_b = (p^3 k\epsilon_0 \mu p)^{1/4} V^{1/2}/(4t)^{3/4}, \tag{3}$$

where $p$, $k$, $\epsilon_0$, $\mu_p$, and $V$ are the volume charge density of the lithium in $WO_3$, the relative dielectric constant of $WO_3$, the dielectric constant in vacuum, the $Li^+$ mobility, and the applied voltage, respectively. This equation shows the bleaching current $J_b$ to be a linear function of $t^{-3/4}$.

Equations (2) and (3), which have been applied to the electrolyte solution system, are used to evaluate the coloring and bleaching mechanism for the ECD system containing polymeric solid electrolyte. The log-log plots for the current of the coloring and bleaching processes versus time are shown in Fig. 10(A) and (B). The slopes of these relationships at steady state are -1/2 and -3/4 for the coloring and bleaching processes, respectively. These results suggest that the coloring and bleaching mechanisms for this all-solid-state ECD can be interpreted, in principle, just like those for ECD cells containing electrolyte solution, and the ion transport across the interface between the $WO_3$ layer and the polymeric solid electrolyte should be effective. Furthermore, it was also clear that the coloring and bleaching mechanisms of the ECD were explained by the barrier-limited current flow [26] in the coloring process, and the space charge-limited current flow of $Li^+$ [27] in the bleaching process, just as for the liquid electrolyte system.

### Application of Single-Ionic Conductor to All-Solid-State Battery

The all-solid-state battery with polymeric solid electrolyte is shown in Fig. 11. The cell preparation has been described in detail [28]. P($MEO_7$-MALi) was used as the solid electrolyte layer for the battery. Metallic lithium and $MnO_2$ were used as active materials for the negative and positive electrodes,

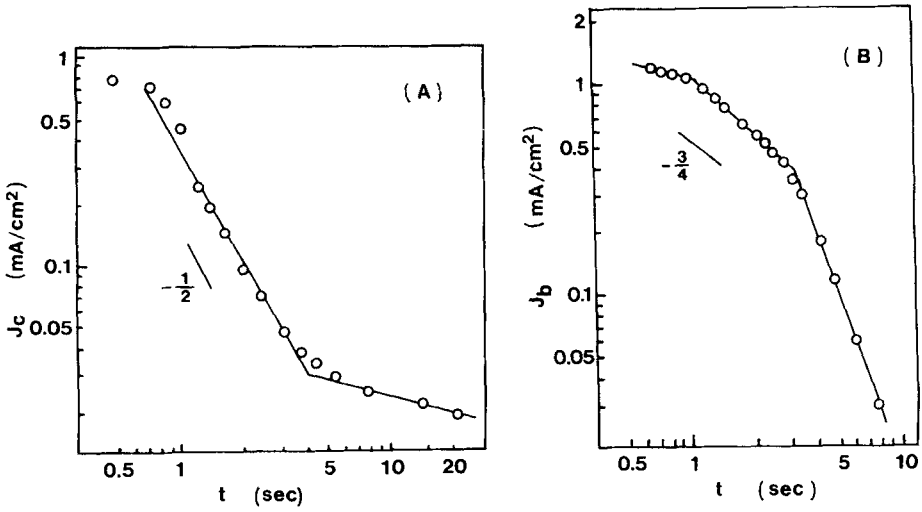


FIG. 10. Log-log plot of current versus time at (A) coloring state and (B) bleaching state.

respectively. A P($MEO_7$-MALi) film was sandwiched between these two electrodes. The thickness of the film was controlled at about 30-50 $\mu$m.

Metallic lithium supplies lithium ions, and these are transferred through the film. $MnO_2$ was selected because this could transfer electrons to the carrier ions easily. The theoretical electromotive force (emf) for a cell constituted of

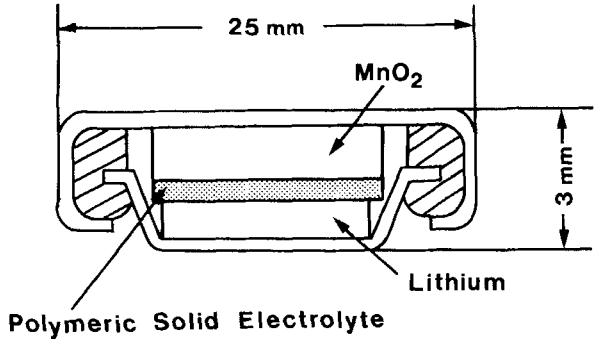


FIG. 11. Cell construction of all-solid-state battery.

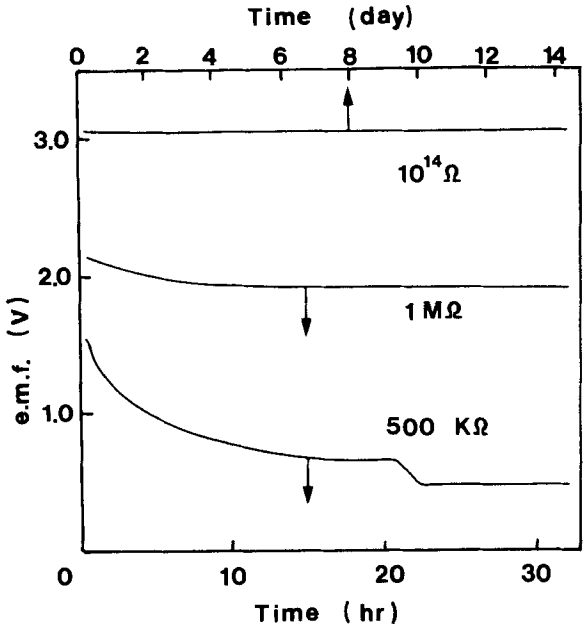


FIG. 12. Discharge curves of the all-solid-state battery.

Li/electrolyte/$MnO_2$ is about 3.5 V. This all-solid-state battery showed an open-circuit voltage $V_{oc}$ of 3.1 V, as shown in Fig. 12. This battery showed a stable emf of 3.1 V for more than 2 weeks at a discharge resistivity of $10^{14}$ Ω because no electronic conduction was concerned. At discharge resistivities of 1 MΩ and 500 kΩ, the emf decreased.

The time dependence of the short-circuit current of the all-solid-state battery with P($MEO_7$-MALi) film is compared with that of the P($MEO_7$)/$LiClO_4$ hybrid film in Fig. 13. For the battery with the P($MEO_7$)/$LiClO_4$ hybrid film, the current decreased at once. In the case of the P($MEO_7$)/$LiClO_4$ hybrid film, anions migrate and accumulate near the anode at short circuit, preventing further supply of lithium ions from the anode and resulting in a decrease of the short-circuit current. On the other hand, for the P($MEO_7$-MALi) film, anion migration should not occur because the anions are covalently bound to the polymer chain. Then, lithium ions are supplied smoothly from the anode to the polymeric solid electrolyte, because there is no carrier sheet formation of anions near the anode. This is the most advanced battery with a single-ionic

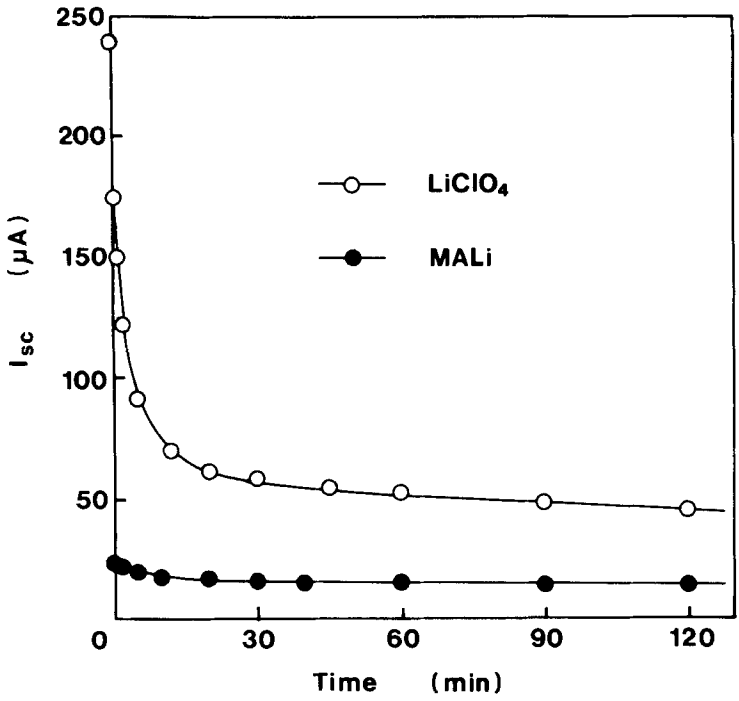


FIG. 13. Time dependence of short circuit current of the all-solid-state battery.



conductive matrix, and it shows excellent time stability for a short-circuit current.

## ACKNOWLEDGMENT

This work was partially supported by a Grant-in-Aid for Scientific Research on Priority Areas "Macromolecular Complexes" from the Ministry of Education, Culture and Science, Japan.

## REFERENCES

[1] E. Tsuchida, H. Ohno, and K. Tsunemi, *Electrochim. Acta, 28,* 591, 833 (1983).

[2] E. Tsuchida, H. Ohno, K. Tsunemi, and N. Kobayashi, *Solid State Ionics, 11,* 227 (1983).
[3] K. Shigehara, N. Kobayashi, and E. Tsuchida, *Ibid., 14,* 85 (1984).
[4] P. V. Wright, *Br. Polym. J., 319,* 137 (1975).
[5] B. L. Papke, M. A. Ratner, and D. F. Shriver, *J. Phys. Chem. Solid, 42,* 493 (1981).
[6] C. Berthier, W. Gorecki, M. Minier, M. B. Armand, J. M. Chabagno, and P. Riguad, *Solid State Ionics, 11,* 91 (1983).
[7] R. Dupon, B. L. Papke, M. A. Ratner, D. H. Whitmore, and D. F. Shriver, *J. Am. Chem. Soc., 104,* 6247 (1982).
[8] J. E. Weston and B. C. H. Steel, *Solid State Ionics, 7,* 81 (1982).
[9] A. Killes, J. F. Le Nest, A. Gandini, and H. Cheradame, *Macromolecules, 17,* 63 (1984).
[10] M. Watanabe, J. Ikeda, and I. Shinohara, *Polym. J., 15,* 65, 175 (1983).
[11] M. Watanabe, K. Sanui, N. Ogata, T. Kobayashi, and Z. Ohtaki, *J. Appl. Phys. 57,* 123 (1985).
[12] L. L. Yang, A. R. McGhie, and G. C. Farrington, *J. Electrochem. Soc., 133,* 1380 (1986).
[13] N. Kobayashi, M. Uchiyama, K. Shigehara, and E. Tsuchida, *J. Phys. Chem., 89,* 987 (1985).
[14] N. Kobayashi, M. Uchiyama, and E. Tsuchida, *Solid State Ionics, 17,* 307 (1985).
[15] N. Kobayashi, T. Hamada, H. Ohno, and E. Tsuchida, *Polym. J., 18,* 661 (1986).
[16] M. Watanabe, M. Rikukawa, K. Sanui, N. Ogata, H. Koto, T. Kobayashi, and Z. Ohtaki, *Macromolecules, 17,* 2902 (1984).
[17] R. Dupon, B. L. Papke, M. A. Ratner, and D. F. Shriver, *J. Electrochem. Soc., 131,* 586 (1984).
[18] C. K. Chiang, G. T. Davis, C. A. Harding, and T. Takahashi, *Macromolecules, 18,* 825 (1985).
[19] S. Clancy, D. F. Shriver, and L. A. Ochrynowycz, *Ibid., 19,* 606 (1986).
[20] N. Kobayashi, H. Ohno, and E. Tsuchida, *Nippon Kagaku Kaishi, 1986,* 441.
[21] K. S. Cole and R. H. Cole, *J. Chem. Phys., 9,* 341 (1941).
[22] M. Watanabe, M. Rikukawa, K. Sanui, and N. Ogata, *J. Appl. Phys. 58,* 736 (1985).
[23] N. Kobayashi, H. Ohno, E. Tsuchida, and R. Hirohashi, *Kobunshi Ronbunshu, 44,* 317 (1987).
[24] N. Kobayashi, H. Ohno, and E. Tsuchida, Unpublished Data.

[25] A. Bouridah, F. Dalard, D. Deroo, and M. B. Armand, *Solid State Ionics, 18/19,* 287 (1986).
[26] S. K. Mohapatra, *J. Electrochem. Soc., 125,* 284 (1978).
[27] B. W. Faughnan, R. S. Crandall, and M. A. Lampert, *Appl. Phys. Lett., 27,* 275 (1975).
[28] H. Ohno, H. Matsuda, K. Mizoguchi, and E. Tsuchida, *Polym. Bull., 7,* 271 (1982).